Dynamic correction for water-velocity and tidal variations

Claudio Guerra, José Carbonesi, Gerson Ritter, Petrobras

Abstract

Water-velocity and tidal variations between sail lines are the main sources of acquisition footprint, especially for deep water surveys, causing unbalanced amplitudes and jittering of reflectors along the crossline direction. These defects can have great impact not only on the final quality of 3D seismic images, but also on 4D studies. Most of the methods aiming at correcting for those variations are static. Some of them propose to be dynamic by using NMO correction, which is an approximation. Here, we use an extrapolation scheme to correct for both variations. Water velocity and a depth-variation parameter are determined via tomographic inversion. Using these parameters, shot gathers are downward extrapolated up to a reference horizon and upward extrapolated back to a constant acquisition surface and using a velocity constant throughout the 3D project. We show promising results on real data.

Introduction

In seismic processing, it is well known that variations of water velocity and sea conditions are the main cause of acquisition footprint, especially for deep water surveys. Unbalanced amplitudes and reflector jittering are the main effects on seismic images, and, sometimes, can impair obtaining a reliable 4D response (Bertrand and MacBeth, 2005). Nowadays, as full waveform inversion is becoming popular, it is common to have those defects imprinted on the final velocity model.

To correct for the effects of water-velocity and tidal variations, a number of methods have been already formulated, ranging from the simple static correction (Wombell, 1997) to dynamic approximations (Fried and MacKay, 2001; Lacombe et al., 2006). These dynamic corrections are called "approximations" because they use NMO to modify traveltimes, not allowing lateral movement of the seismic energy. This approximation is prone to fail in regions where canyons are present or the water bottom has strong dips.

Here, we use wavefield extrapolation implemented on GPU´s to overcome the limitations presented by static and NMO-based dynamic corrections. The method is fully 3D and uses an estimate of the water bottom in depth, of the water velocity, and of the tidal variations. The last two are computed by tomography (Ritter, 2010). We discuss the theory and show tests on synthetic and field data, which results are promising.

Theory

We use the phase-shift extrapolator to perform water-velocity and tidal corrections. Water velocity and a vertical displacement related to tides or waves are determined by tomography, following the work of Ritter (2010).

Shot gathers can be mathematically described in the frequency domain by

$$d(\mathbf{x_s}, \mathbf{x_r}; \omega) = \int_A G_D(\mathbf{x_s}, \mathbf{x}; \omega) r(\mathbf{x}) G_U(\mathbf{x}, \mathbf{x_r}; \omega) d\mathbf{x} \quad , (1)$$

considering a Delta function as input. In equation 1, ω is the radial frequency; $\mathbf{x_s}$, $\mathbf{x_r}$, and $\mathbf{x}$ are shot, receiver, and model position vectors, respectively. In the present case, G_D is the downgoing one-way Green´s function and G_U is the upgoing one-way Green´s function, *r* is the reflectivity, and A is the experiment aperture.

To compute what would be the data $\widetilde{d}$ if $\mathbf{x_s}, \mathbf{x_r}$ where positioned on the water bottom $\widetilde{\mathbf{x}}$, we use

$$\widetilde{d}(\widetilde{\mathbf{x}}; \omega) = \int G_U{}^*(\mathbf{x_r}, \widetilde{\mathbf{x}}; \omega) d\mathbf{x_r} \int G_D{}^*(\mathbf{x_s}, \widetilde{\mathbf{x}}; \omega) d(\mathbf{x_s}, \mathbf{x_r}; \omega) d\mathbf{x_s} \quad . (2)$$

The downgoing Green´s functions are computed using the tomographic estimation of the propagation velocity. The asterisk denotes complex conjugate. Notice that the double integration corresponds to a survey-sinking scheme, in which wavefields should be sorted to shot and receiver domains prior to propagation at every depth step. Since this scheme is cumbersome, a more common strategy is to recast the problem in the midpoint-offset domain. However, these solutions are inadequate for the problem we are solving because in both we mix water velocities and vertical displacements for different shots. We overcome this limitation by using the shot-profile scheme and by extrapolating only the receiver wavefield up to a modified water bottom, $\widetilde{\mathbf{x}}^*$. So, the data $\widetilde{d}$ now reads

$$\widetilde{d}(\widetilde{\mathbf{x}}^*; \mathbf{x_s}, \omega) = \int G_D{}^*(\mathbf{x_r}, \widetilde{\mathbf{x}}^*; \omega) d(\mathbf{x_s}, \mathbf{x_r}; \omega) d\mathbf{x_r} \quad . (3)$$

For a dipping water bottom, the modified water bottom $\widetilde{\mathbf{x}}^*$, corresponds to doubling the dip.

Using the same extrapolation strategy, to compute the corrected data d_{corr}, we need to extrapolate back $\widetilde{d}$ with a single velocity for the entire survey and collecting them at a depth which takes into account the vertical displacement caused by tides or waves, according to

$$d_{corr}(\mathbf{x_s}, \mathbf{x_r}; \omega) = \int G_{Dcorr}(\widetilde{\mathbf{x}}^*, \mathbf{x_r}; \omega) \widetilde{d}(\widetilde{\mathbf{x}}^*; \mathbf{x_s}, \omega) d\widetilde{\mathbf{x}}^* \quad , (4)$$

where G_{Dcorr} is computed with a constant water velocity, say 1,500 m/s.

Next, we illustrate the method on synthetic data.

Examples

Firstly, to test our strategy, we modeled 50 shots on a 2.5D model with two dipping reflectors. These shots, fired on the same crossline but on different inlines, would correspond to a 3D acquisition geometry of only one cable per shot. Water velocity randomly varied with values of 1,480 m/s, 1,500 m/s, 1,520 m/s, and 1,540 m/s (Figure 1a). Tidal- and wave-related displacements also are randomly distributed between -5 m and 4 m (Figure 1b). It is worth mentioning that these values are not frequently found along the same survey, therefore we are pushing the example to the limits. Figure 2 shows two different common-offset sections, in which is clear the effect of the variation of the two parameters on the data.

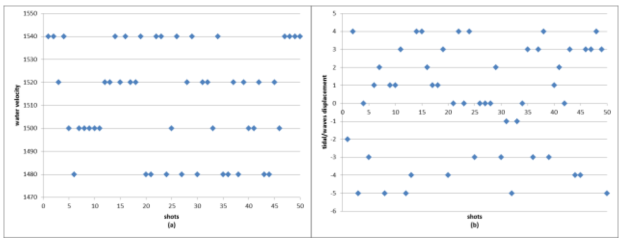

Figure 1 – Water velocity (a) and tidal/waves related displacement (b) values used in the modeling.

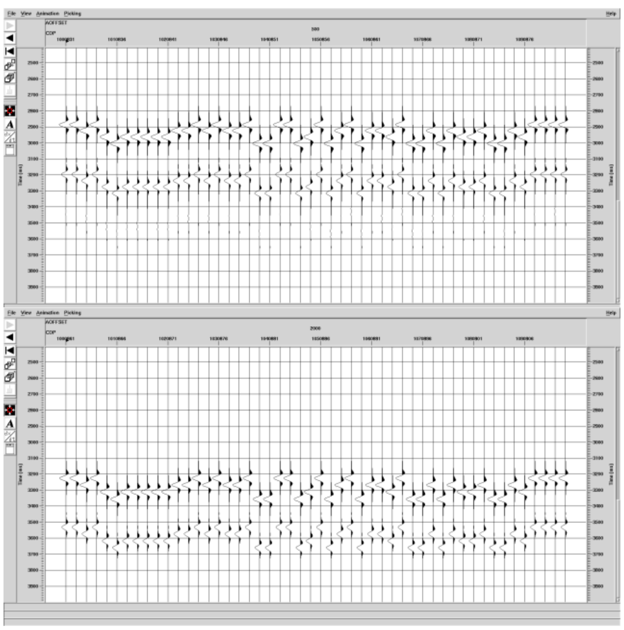

Figure 2 – Two input common offset panels, corresponding to different crosslines along the 3D synthetic data. Top: 500 m; bottom: 2,000 m.

By applying our method on the data of Figure 2 we obtain aligned reflections (Figure 3).

Results

Now, we show how the method performs on conventional streamer real data. We use some sail lines of a 3D survey in the Santos Basin, Brazil. Water depth is about 2,100 m. Similarly to the synthetic example, shot points were selected from the sail lines, in such a way that selecting a given offset bin corresponds to selecting a crossline.

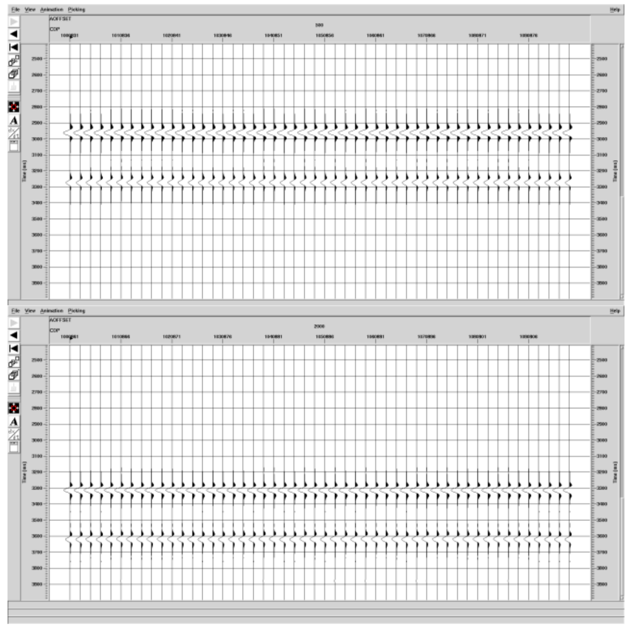

Figure 3 – Two corrected common offset panels, corresponding to different crosslines along the 3D synthetic data. Top: 500 m; bottom: 2,000 m.

The horizon corresponding to the water bottom was interpreted on a post-stack depth migrated volume and it was smoothed to eliminate acquisition related variations. Figure 4 shows this horizon before and after edition and the difference between them, highlighting the acquisition footprint. The difference map ranges from –16 to +16 meters. Crosslines are in the NS direction, perpendicular to the stripes in the difference map. The edited version is used as input to compute water velocity and the vertical displacement by tomography, as well as in the water correction itself.

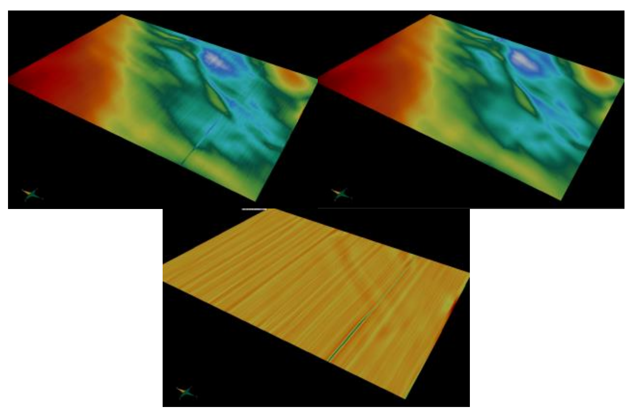

Figure 4 – Water bottom before edition (top left), after edition (top right), and difference (bottom).

In Figure 5, we display offset bins, nearly corresponding to different crosslines, of the real data input to correction and, in Figure 6, the results for the same offset bins as those of Figure 5. Figures 7 and 8 shows zoomed views in regions where corrections were more critical. Notice the better continuity of reflectors from top to bottom.

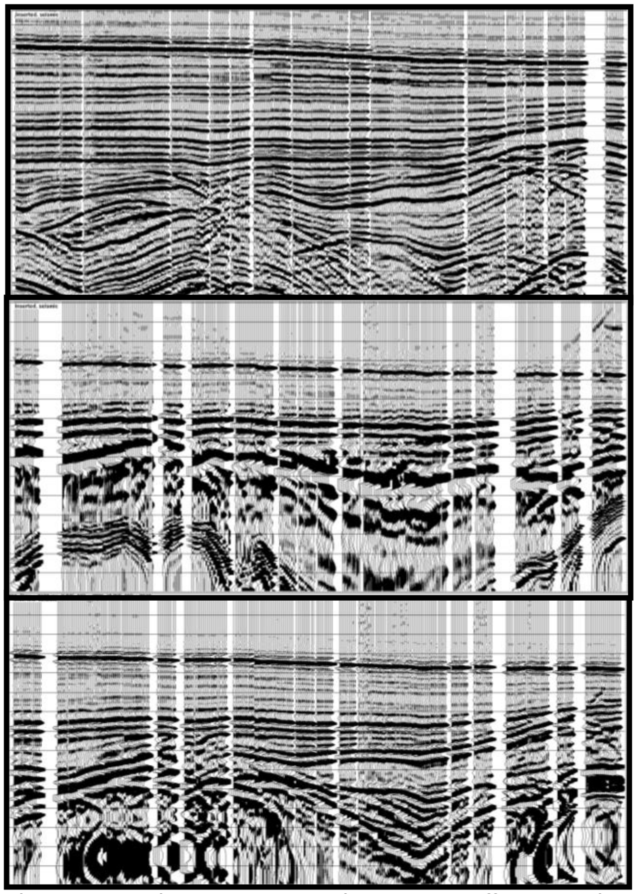

Figure 5 – Three uncorrected common offset panels, corresponding to different crosslines along the 3D real data. Top: 1,500 m; middle: 5,720 m; bottom: 4,630 m.

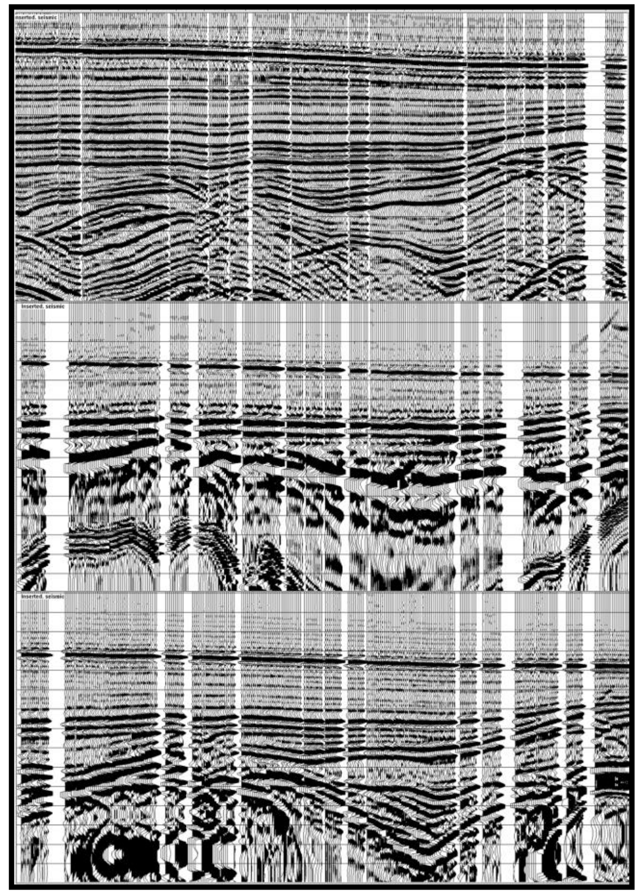

Figure 6 – Three corrected common offset panels, corresponding to different crosslines along the 3D real data. Top: 1,500 m; middle: 5,720 m; bottom: 4,630 m.

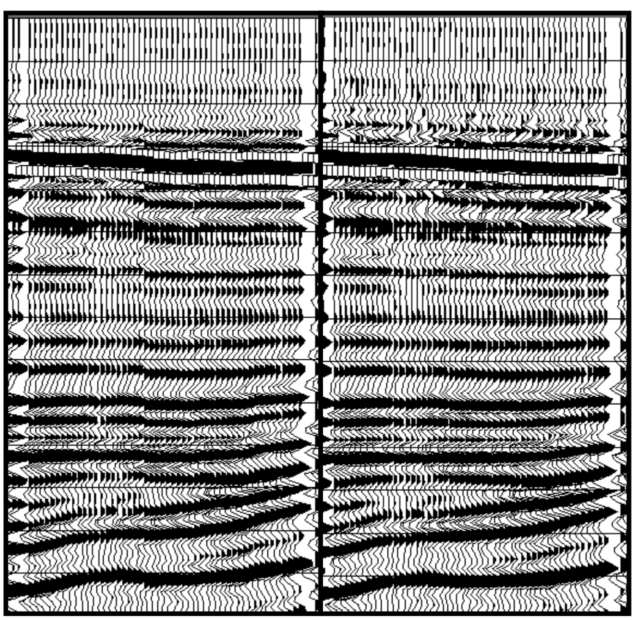

Figure 7 – Zoomed view of the 1,500 m offset panel, showing better continuity of reflections. Before (left) and after (right) correction.

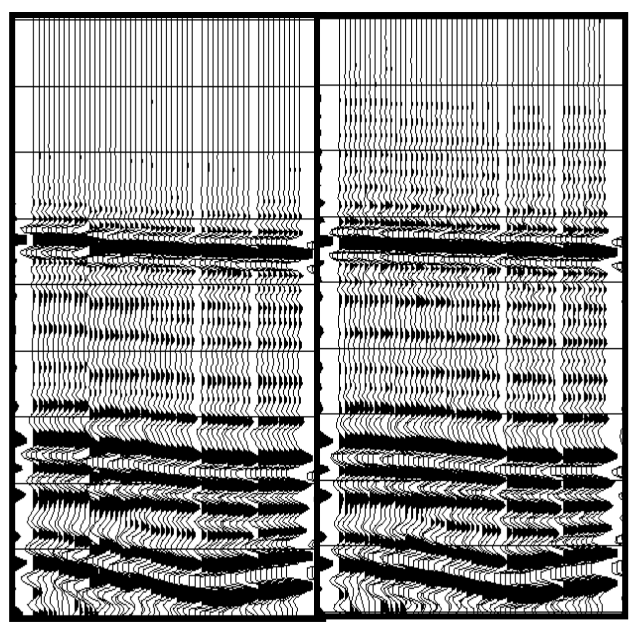

Figure 8 – Zoomed view of the 4,630 m offset panel, showing better continuity of reflections. Before (left) and after (right) correction.

Conclusions

We achieve efficient dynamic correction for water-velocity and tidal variations by wavefield propagation. Data are downward extrapolated in the shot domain, using an estimated water velocity and vertical displacement computed by tomography. Then, an upward extrapolation with a constant velocity brings data to the same water conditions. Results on real data are promising.

Acknowledgments

We would like to acknowledge Petrobras for allowing publication.

References

Wombell, R., 1997, Water velocity variations and static corrections in 3D data processing, 59th Internat. Mtg: Eur. Assn. Geosci. Eng., A029.

Fried, J. and S.MacKay, 2001, Dynamic corrections for water velocity variations: A Nova Scotia case history, CSEG.

Lacombe, C., J. Schultzen, S. Butt and D. Lecerf, 2006, Correction for Water Velocity Variations and Tidal Statics, 68th EAGE Conference and Exhibition incorporating SPE EUROPEC 2006

Ritter, G., 2010, Water velocity estimation using inversion methods, Geophysics, v. 75, p. U1-U8.

Bertrand, A. and C. MacBeth, 2005, Repeatability enhancement in deep-water permanent seismic installations: a dynamic correction for seawater velocity variations, Geophysical Prospecting, 2005, 53, 229–242